APPENDIX A
THE EVT HEV MODEL

A. Kinematics Model

The kinematics model is developed by combining all of the masses and gears in the system. All shafts are assumed infinitely stiff. The kinematics of the Dual-Mode EVT (DMEVT) are illustrated in Figure 1. The dynamics and modeling of a DMEVT are thoroughly developed and discussed in [1]. The term dual-mode refers to the use, in operation, of two clutch configurations, or modes, in the transmission. When the transmission is combined with the rest of the powertrain and vehicle, the resulting system can be represented using lever diagrams [2] as in Figure 2. Since the clutches are no slip, or dog clutches, the clutches are locked or open. The clutches never pass torque while slipping. Hence, the clutches in the transmission allow for four possible discrete states for this system. For modeling simplification, the transient mode with both clutches open is ignored by the high-level control. The mode with both clutches closed locks the transmission; therefore this combination is not used. This leaves two modes. In each of these modes, the transmission has two degrees of freedom which permit the engine speed, ω_e, and vehicle speed, v_{veh}, to behave independently. In other words, for any given vehicle speed, the engine speed can take any feasible value.

The model of the kinematics uses two matrices, $K_{kine,\Delta}$ and $K_{kine,r}$. $K_{kine,\Delta}$ represents the relation between torque and speed change. $K_{kine,r}$ contains the speed ratios between components. The matrices are developed from the lever diagram using a ring to sun ratio of 2 for both planetary gears in the transmission. There is a torque efficiency of 99% associated with all torque passing between the electric machines and the transmission. The final drive ratio is 3.55 and the tire radius is 0.377 meters. The vehicle has a mass of 2000 kg, the engine has an inertia of 0.115 kg-m^2. Both electric machines have an inertia of 0.052 kg-m^2. All other inertias are assumed negligible. See Table 1 for the values of $K_{kine,\Delta}$ and $K_{kine,r}$ in each clutch mode.

Using these matrices, the model of the kinematic dynamics, in discrete time is

$$\begin{bmatrix} v_{veh} & \omega_e \end{bmatrix}_{next}^T = \begin{bmatrix} v_{veh} & \omega_e \end{bmatrix}^T + \left[K_{kine,\Delta}\left(C_1, C_2\right)\right] \cdot \left(T_v + T_{losses}\right). \quad (1)$$

The vector T_v contains the torques that can be controlled. This vector is

$$T_v = \begin{bmatrix} T_e & T_A & T_B & T_k \end{bmatrix}^T. \quad (2)$$

The vector T_{losses} is comprised of the assorted torque losses in the system and is defined as

$$T_{losses} \triangleq \begin{bmatrix} T_{loss,e} & T_{loss,A} & T_{loss,B} & T_{loss,out} & F_v \end{bmatrix} \quad (3)$$

where $T_{loss,e}$ is the net torque losses experienced at the engine shaft on the transmission, $T_{losses,A}$ is the net torque losses experienced at the transmission shaft associated with motor A, $T_{losses,B}$ is the same for motor B and $T_{loss,out}$ is the effective torque loss on the output shaft. Finally, F_v is the net force applied to the vehicle body. These losses are determined within the transmission model and vehicle model based on the speeds of various nodes in the kinematic model. Given the engine speed and the vehicle speed, the speed of all other components of interest in the model is computed using

$$\begin{bmatrix} \omega_A & \omega_B & \omega_{FD} & \omega_{out} \end{bmatrix}^T = \left[K_{kine,r}\left(C_1, C_2\right)\right] \cdot \begin{bmatrix} \omega_e & v_{veh} \end{bmatrix}^T \quad (4)$$

B. Vehicle and Final Drive Ratio Model

The vehicle is modeled as a unicycle without tire slip or weight transfer. The inertia associated with the vehicle is integrated into the kinematic model. The losses modeled include the final drive ratio losses. The force applied to the vehicle are modeled as

$$F_v = F_0 \cdot \operatorname{sgn}(v) + F_1 \cdot v + F_2 \cdot v^2. \quad (5)$$

The vehicle speed is limited to between zero and $v_{veh,\max}$. The torque applied by the chassis brake is limited to a maximum of $T_{k,\max}$. The chassis brake cannot apply torque to accelerate the vehicle. These limits are expressed in negative null form as

$$g_{vehicle}\left(x, v\right) = \begin{bmatrix} -v_{veh} \\ v_{veh} - v_{veh,\max} \\ T_{k,\min} - T_k \\ T_k \end{bmatrix} \le 0. \quad (6)$$

C. Engine Model

The engine model is based on a Willan's Line model, similar to [3, 4]. The engine is modeled as thermally stable. Because the engine speed is modeled as part of the kinematics, (1), there are no states associated with the rest of the engine model. Let s be the mean piston speed:

$$s = S \cdot \omega_e / \pi, \quad (7)$$

where S is the piston stroke and ω_e is engine speed in radians per second. Let P_m be the mean effective pressure on the piston:

$$P_m = \left(4 \cdot \pi \cdot Q_{LHV} \cdot W_f\right) / \left(V_d \cdot \omega_e\right), \quad (8)$$

where Q_{LHV} is the lower heating value of the fuel, W_f is the fuel flow and V_d is the engine displacement. The brake torque, T_{brk} produced by the engine is modeled as

$$\begin{aligned} \left(4 \cdot \pi \cdot T_{brk} / V_d\right) &= \left(a_{00} + a_{01} \cdot s + a_{02} \cdot s^2\right) \cdot P_m \\ &\quad - \left(a_{10} + a_{11} \cdot s\right) \cdot P_m^2 - \left(p_{mr0} + p_{mr2} \cdot s^2\right) \end{aligned} \quad (9)$$

In this model, the coefficients a_{xx} parameterize the speed dependence of the fuel to engine power conversion. The coefficients p_{mrx} parameterize the frictional losses in the engine. The units and values of the parameters are summarized in Table 1. Since the engine brake torque is an input, engine fuel flow is found by using the quadratic equation to explicitly find W_f as a function of T_{brk} and ω_e.

The maximum engine torque is modeled as

$$T_{e,\max} = \begin{cases} K_{T,0} + K_{T,1} \cdot \omega_e + K_{T,2} \cdot \omega_e^2 & ,\text{if } \omega_e > 0 \\ 0 & ,\text{otherwise} \end{cases}, \tag{10}$$

where $K_{T,x}$ are coefficients that characterize the torque curve. The minimum engine torque, $T_{e,\min}$, is zero. The BSFC and peak torque curves are plotted in Figure 3.

If the engine is off, with a speed of zero, it is assumed to instantaneously transition to an idle speed specified by $\omega_{e,start}$ when it is started. If it is turned off, it is assumed to instantaneously transition to zero speed. In both cases, it is assumed negligible fuel and battery energy are involved. If M_e indicates the engine should be running, then the engine is restricted to operate between $\omega_{e,\min,0}$ and $\omega_{e,\max,0}$. Otherwise the engine is restricted to zero speed. These constraints are summarized as

$$\omega_{e,\max} = \begin{cases} 0 & ,\text{if } M_e = '\mathit{off}' \\ \omega_{e,\max,0} & ,\text{if } M_e = '\mathit{run}' \end{cases}, \tag{11}$$

and

$$\omega_{e,\min} = \begin{cases} 0 & ,\text{if } M_e = '\mathit{off}' \\ \omega_{e,\min,0} & ,\text{if } M_e = '\mathit{run}' \end{cases}. \tag{12}$$

Since the goal of this model is to understand the value of using SDP to reduce fuel consumption and emissions, the engine out emissions in the model are normalized and assumed proportional to fuel flow:

$$W_{e,eng} \triangleq W_f \,. \tag{13}$$

The fuel control is assumed sufficiently accurate that changes in engine operation do not increase engine out emissions. This simplifies the model and the interpretation of the benefits of SDP in improving emissions.

Finally, the exhaust gas temperature, T_{exh}, is modeled as tracking the power level in the engine with a maximum temperature as

$$T_{exh} = \min\left(343, 315 + 49 \cdot W_f\right) \tag{14}$$

in units of degrees Celsius. The exhaust gas temperature is assumed to change instantaneously.

The constraints on engine operation are summarized in negative null form [5] as

$$g_{engine}(x,v) = \begin{bmatrix} T_e - T_{e,\max} \\ T_{e,\min} - T_e \\ \omega_{e,next} - \omega_{e,\max} \\ \omega_{e,\min} - \omega_{e,next} \end{bmatrix} \le 0 \,. \tag{15}$$

The minimum speed used in this model was the engine idle speed. However, speeds other than the idle speed of the engine can be used. Furthermore, the minimum and maximum torques used in this model were limited by the engine capabilities. In many situations considerations such as engine noise and vibration would limit the operating area well within the physical capability of the engine.

For this model, the engine was assumed to accelerate only as limited by the torque applied to the engine mass. In many cases, there are limits on the acceptable acceleration and this can limit can modeled by introducing an explicit constraint on engine acceleration.

D. Catalyst Model

Many models of automotive catalysts have been developed. These models incorporate chemical reactions and thermal behavior. The types of models range from partial differential equation and finite element based [6-11] to simpler control oriented models [12-16]. The primary focus of these models is on the chemical reactions inside that catalyst. Specific pollutants are not modeled. Instead, the catalyst conversion efficiency is simplified to a temperature dependent curve roughly fit to published curves on catalyst efficiency with respect to temperature in [17]. The resulting efficiency model for the catalyst depends on the sole state variable for the catalyst, T_{cat}, and is

$$\eta_{cat} = \min\left(0.99, \max\left(0, 0.5 + 1.07 \cdot \tan^{-1}\left(\frac{9 \cdot T_{cat} - 415}{125 \cdot \pi}\right)\right)\right). \tag{16}$$

The normalized tailpipe emissions are

$$W_e = \left(1 - \eta_{cat}\right) \cdot W_{e,eng} \,. \tag{17}$$

Many control oriented models [12-14, 18] make the assumption that there is no heat transfer to the ambient environment and the primary sources of heat are the exhaust gas and internal conversion of the pollutants. However, even in still air, there is under hood and underbody heat transfer to the ambient environment [19]. When the vehicle is in motion this heat transfer will be greater due to forced convection. In many applications, this heat transfer is negligible. However with strong and charge depleting hybrids, where the engine may be off an appreciable period of time, heat transfer can impact emissions. The change in temperature due to heat transfer to the environment is modeled as

$$dT_{cat-amb} = \left(T_{cat} - T_{amb}\right) \cdot \left(1 - e^{\left(-1/\tau_{cat-amb}\right)}\right). \tag{18}$$

The ambient temperature, T_{amb}, is assumed to be 21 degrees Centigrade. The coefficient $\tau_{cat-amb}$ is the time constant associated with cooling of the catalyst to the ambient environment. The change in temperature due to heat transfer from the exhaust gas is modeled as

$$dT_{cat-exh} = \begin{cases} \left(T_{cat} - T_{exh}\right) \cdot \left(1 - e^{\left(-1/\tau_{cat-exh}\right)}\right) & ,\text{if } W_f > 0 \\ 0 & ,\text{otherwise} \end{cases}. \tag{19}$$

In the case that the engine is off, $W_{e,eng} = 0$, all heat transfer from the exhaust gases is assumed to stop. The coefficient $\tau_{cat-exh}$ is selected based on the model in [13] and set to 24.5. To simplify the issues with catalyst light off, the catalyst is assumed to always be lit and converting pollutants. It is assumed that heat is released in proportion to the fraction of pollutants converted and change in temperature is modeled as

$$dT_{cat-conv} = \eta_{cat} \cdot W_{e,eng} \cdot K_{cat,conv} \tag{20}$$

where $K_{cat,conv}$ is 6.1e-3. These contributions to changes in catalyst brick temperature are combined to obtain the temperature difference equation

$$T_{cat,next} = T_{cat} + dT_{cat-conv} + dT_{cat-exh} + dT_{cat-amb} \,. \tag{21}$$

To prevent catalyst damage, the catalyst maximum temperature is limited. The control constraint on catalyst operation is

$$g_{catalyst}(x,v) = \left[T_{cat} - T_{cat,\max}\right] \le 0 \,. \tag{22}$$

E. Transmission Model

The dynamic associated with the transmission are integrated into the kinematic model. The algebraic model for the transmission model includes the spin losses associated with the motors. These spin losses are the effective loss at the transmission input from the engine,

$$T_{loss,e} = -\begin{pmatrix} K_{D,e,0}(C_1,C_2) + K_{D,e,1}(C_1,C_2)\cdot\omega_e \\ +K_{D,e,out}(C_1,C_2)\cdot\omega_{out} \end{pmatrix}; \tag{23}$$

the effective losses at the motor A input to the transmission,

$$T_{loss,A} = -\left(K_{D,A,0} + K_{D,A,1}\cdot|\omega_A|\right)\cdot \operatorname{sgn}(\omega_A)\,; \tag{24}$$

the effective losses at the motor B input to the transmission,

$$T_{loss,B} = -\left(K_{D,B,0} + K_{D,B,1}\cdot|\omega_B|\right)\cdot \operatorname{sgn}(\omega_B)\,; \tag{25}$$

and the effective losses at the output of the transmission,

$$T_{loss,out} = -\begin{pmatrix} K_{D,out,0}(C_1,C_2) + K_{D,out,1}(C_1,C_2)\cdot\omega_{out} \\ +K_{D,out,e}(C_1,C_2)\cdot\omega_e \end{pmatrix}. \tag{26}$$

When the clutches in the transmission change their configuration, this is referred to as a mode change. In a full model, this process would be modeled to include a transient through a state where both clutches are open. In this configuration, since no-slip clutches are used, the engine and electric machine torques are used to change the speeds of motor A and motor B so closing clutch face speed goes to zero. For this simple model, this complex process is ignored by assuming the change is instantaneous and a negligible amount of energy is involved. The clutch commands are received as inputs and instantaneously resolved as

$$M_{trans} = \begin{cases} 1 & ,\text{if } C_{1,cmd} = 1 \;\&\; C_{2,cmd} = 0 \\ 2 & ,\text{if } C_{1,cmd} = 0 \;\&\; C_{2,cmd} = 1 \end{cases}. \tag{27}$$

During the mode change, the engine speed and vehicle speeds remain constant through the change, so the speeds of motor A and motor B are recalculated using (4).

F. Electric Machine and Inverter Model

Each electric machine and its inverter are lumped into an algebraic model,

$$P_{motx} = \left(T_x + T_x^2\cdot K_{motx,2}\right)\cdot\omega_x\,, \tag{28}$$

where T_x is the mechanical torque impressed on the rotor, ω_x is the speed of that rotor, $K_{motx,2}$ is a quadratic loss coefficient and the symbol x indicates motor A or B. As noted previously, the dynamics associated with the motors' inertia are lumped into the kinematic model and the spin losses associated with the electric machines are lumped into the transmission model.

The electric machines are limited by power and torque. Specifically, each machine's maximum torque is

$$T_{x,\max} = \min\left(T_{x,\max,0}, \frac{P_{x,\max}}{\left(|\omega_x| + \varepsilon\right)}\right), \tag{29}$$

and minimum torque is

$$T_{x,\min} = \min\left(T_{x,\min,0}, \frac{P_{x,\min}}{\left(|\omega_x| + \varepsilon\right)}\right). \tag{30}$$

These constraints on torque are combined to define the motors constraints,

$$g_{motors}(x,v) = \begin{bmatrix} T_A - T_{A,\max} \\ T_{A,\min} - T_A \\ T_B - T_{B,\max} \\ T_{B,\min} - T_B \end{bmatrix} \le 0 \tag{31}$$

G. Battery Model

The battery model is a simplified ohmic battery based on the model in [20]. This simplified model consists of an ideal voltage source in series with an ohmic resistor. The voltage source is equal to the open circuit voltage measured on the battery. The ohmic resistance is constant and is fit to the change in terminal voltage divided by the change in terminal current. Both of these terms are modeled as invariant to changes in battery state of charge.

The dynamics of the battery are associated with the change in battery state of charge. This is modeled as an ideal discrete time integrator:

$$q_{batt,next} = q_{batt} + \left(I_{batt}/Q_{batt}\right)\cdot\Delta t\,. \tag{32}$$

The current is determined by first finding the total power on the terminals of the battery. This total power consists of motor A power, motor B power and other power loads on the vehicle.

$$P_{batt} = P_{motA} + P_{motB} + P_{misc}\,. \tag{33}$$

Using the ohmic battery model, the terminal voltage on the battery is

$$V_{batt,term} = V_{batt,OC} + I_{batt}\cdot R_{batt}\,. \tag{34}$$

The power at the terminals of the battery is

$$P_{batt} = V_{batt,term}\cdot I_{batt}\,. \tag{35}$$

The battery current is found by substituting (34) into (35) and using the quadratic equation to solve for I_{batt}.

The battery power limit is constrained between $P_{batt,\min}$ and $P_{batt,\max}$. The state of charge of the battery is limited between $q_{batt,\min}$ and $q_{batt,\max}$. The constraints on the battery are

$$g_{battery}(x,v) = \begin{bmatrix} P_{batt} - P_{batt,\max} \\ P_{batt,\min} - P_{batt} \\ q_{next} - q_{batt,\max} \\ q_{batt,\min} - q_{next} \end{bmatrix} \le 0 \tag{36}$$

H. Model Parameters

Table 1 - Model Parameters, Values, and Units (1)

Model Parameter	Nominal Value	Units
a_{00}	0.33	N-m-s/W
a_{01}	0.016	N-s^2/W
a_{02}	-0.0007	N-s^3/(m-
a_{10}	-8.4435e-6	N-m^4-
a_{11}	1.9481e-6	N-m^3-
F_0	138	N
F_1	0.475	N/m/s
F_2	0.56	N/(m/s)^2
J_A	0.052	Kg-m^2
J_B	0.052	Kg-m^2
$K_{cat,conv}$	6.1e-3	C-s/g
$K_{D,A,0}$	0.76	N-m
$K_{D,A,1}$	1.24e-3	N-m-s/rad
$K_{D,B,0}$	0.76	N-m
$K_{D,B,1}$	1.24e-3	N-m-s/rad
$K_{D,e,0}(1,0)$	4.2242	N-m
$K_{D,e,0}(0,1)$	5.0681	N-m
$K_{D,e,1}(1,0)$	0.0212	N-m-s/rad
$K_{D,e,1}(0,1)$	0.0685	N-m-s/rad
$K_{D,e,out}(1,0)$	-0.0396	N-m-s/rad
$K_{D,e,out}(0,1)$	-0.0584	N-m-s/rad
$K_{D,out,0}(1,0)$	0.0000	N-m
$K_{D,out,0}(0,1)$	0.000	N-m
$K_{D,out,1}(1,0)$	1.5669	N-m-s/rad
$K_{D,out,1}(0,1)$	0.6648	N-m-s/rad
$K_{D,out,e}(1,0)$	-0.4115	N-m-s/rad
$K_{D,out,e}(0,1)$	-0.6024	N-m-s/rad
$K_{kine,r}(1,0)$	$\begin{bmatrix} 3.0000 & -56.4987 \\ 0.0000 & 28.2493 \end{bmatrix}$	
$K_{kine,r}(0,1)$	$\begin{bmatrix} -1.0000 & 18.8329 \\ 2.0000 & -9.4164 \end{bmatrix}$	

Table 2 - Model Parameters, Values, and Units (2)

Model Parameter	Nominal Value	Units
$K_{kine,\Delta}(1,0)$	$\begin{bmatrix} 1.5771 & 0.0073 \\ 4.2948 & -0.0049 \\ 0.2064 & 0.0134 \\ 0.0691 & 0.0045 \end{bmatrix}^T$	
$K_{kine,\Delta}(0,1)$	$\begin{bmatrix} 2.0773 & 0.0027 \\ -2.0151 & 0.0065 \\ 0.2064 & 0.0009 \\ 4.1080 & 0.0046 \end{bmatrix}^T$	
$K_{motA,2}$	0.0003	W-s/N^2-m^2-rad
$K_{motB,2}$	0.0003	W-s/N^2-m^2-rad
$K_{T,0}$	191.94	N-m
$K_{T,1}$	0.9153	N-m-s/rad
$K_{T,2}$	-0.0011	N-m-(s/rad)^2
$P_{A,\max}$	65	kW
$P_{B,\max}$	65	kW
p_{mr0}	125.3041	N/m^2
p_{mr2}	0.4549	N-s^2/m^4
P_{misc}	0	W
Q_{batt}	36,000	A-s
Q_{LHV}	44,000	J/g
S	0.086	m
$T_{A,\max,0}$	300	N-m
$T_{B,\max,0}$	300	N-m
$T_{cat,\max}$	650	C
$T_{k,\min}$	-10,000	N-m
V_0	300	V
V_d	0.0038	m^3
$v_{veh,\max}$	45	m/s
$\tau_{cat-amb}$	$\{\infty, 1725, 40\}$	s
$\tau_{cat-exh}$	24.5	s
$\omega_{e,\max,0}$	100	rad/s
$\omega_{e,\min,0}$	600	rad/s
$\omega_{e,start}$	200	rad/s

REFERENCES

[1] D. Zhang, J. Chen, T. Hsieh, J. Rancourt, and M. R. Schmidt, "Dynamic Modeling and Simulation of Two-Mode Electric

Variable Transmission," *Proceedings of the Institute of Mechanical Engineers,* vol. 215 Part D, pp. 1217-1223, 2001.

[2] H. L. Benford and M. B. Leising, "The level analogy: A new tool in transmission analysis," *SAE Paper No. 810102,* 1981.

[3] V. H. Mucino, W. G. Wang, and J. E. Smith, "Parametric Modeling of Internal Combustion Engine Systems for Design Optimization," *SAE Paper No. 904780,* 1990.

[4] J. M. Novak and P. N. Blumberg, "Parametric simulation of significant design and operating alternatives affecting the fuel economy and emissions of spark-ignited engines," *SAE Paper No. 780943,* 1978.

[5] P. Y. Papalambros and D. J. Wilde, *Principles of Optimal Design: Models and Computation*, 2 ed. New York, New York: Cambridge University Press, 2000.

[6] S. Büchner, S. S. Lardies, A. Degen, A. Donnerstag, and W. Held, "A Modular Numerical Simulation Tool Predicting Catalytic Converter Light-Off by Improved Modeling of Thermal Management and Conversion Characteristics," *SAE Paper No. 2001-01-0940,* 2001.

[7] C. Depcik and D. Assanis, "One-dimensional automotive catalyst modeling," *Progress in Energy and Combustion Science* vol. 31, pp. 308-369, 2005.

[8] C. D. Depcik,"Modeling Reacting Gases and Aftertreatment Devices for Internal Combustion Engines," Ph.D. dissertation, Dept of Mechanical Engineering, University of Michigan, Ann Arbor, Michigan, 2003.

[9] J. Kallenbach, P. Flörchinger, and A. Heibel, "Modeling of Automotive Aftertreatment Catalysts," *SAE Paper No. 1999-01-3043,* 1999.

[10] E. R. Becker, R. Watson, M. Brayer, C. Vogt, and M. Makino, "Prediction of catalytic performance during light-off phase with different wall thickness, cell density and cell shape," *SAE Paper No. 2001-01-0930,* 2001.

[11] P. M. Laing, M. D. Shane, S. Son, A. A. Adamczyk, and P. Li, "A simplified approach to modeling exhaust system emissions: SIMTWC," *SAE Paper No. 1999-01-3476,* 1999.

[12] B. T. Shaw, II,"Modeling and Control of Automotive Coldstart Hydrocarbon Emissions," Ph.D. dissertation, Dept. of Mechanical Engineering, University of California, Berkley, Berkley, CA, 2002.

[13] E. P. Brandt, Y. Wang, and Jessy W. Grizzle, "Dynamic Modeling of a Three-Way Catalyst for SI Engine Exhaust Emission Control," *IEEE Transactions on Control Systems Technology,* vol. 8, pp. 767-776, September 2000.

[14] E. P. Brandt,"Modeling and Diagnostics of Three Way Catalysts for Advanced Emissions Control Systems," Ph.D. dissertation, Dept. of Electrical Engineering: Systems, University of Michigan, Ann Arbor, Michigan, 1998.

[15] P. R. Sanketi, J. C. Zavala, and J. K. Hedrick, "Automotive Engine Hybrid Modeling and Control for Reduction of Hydrocarbon Emissions," *International Journal of Control,* vol. 79, pp. 449-464, May 2006.

[16] J. C. P. Jones and K. R. Muske, "Model-based OBD for three-way catalyst systems," *SAE Paper No. 2004-01-0639,* 2004.

[17] R. M. Heck and R. J. Farrauto, *Catalytic Air Pollution Control: Commercial Technology*. New York, N.Y.: Van Nostrand Reinhold, 1995.

[18] B. T. Shaw, II and J. K. Hedrick, "Closed-Loop Engine Coldstart Control to Reduce Hydrocarbon Emissions," in *American Control Conference*, Denver, Colorado, 2003, pp. 1392-1397.

[19] D. Klein and W. K. Cheng, "Spark Ignition Engine Hydrocarbon Emissions Behaviors in Stopping and Restarting," *SAE Paper No. 2002-01-2804,* 2002.

[20] "FreedomCAR Battery Test Manual for Power-Assist Hybrid Electric Vehicles," Department of Energy, October, 2003.

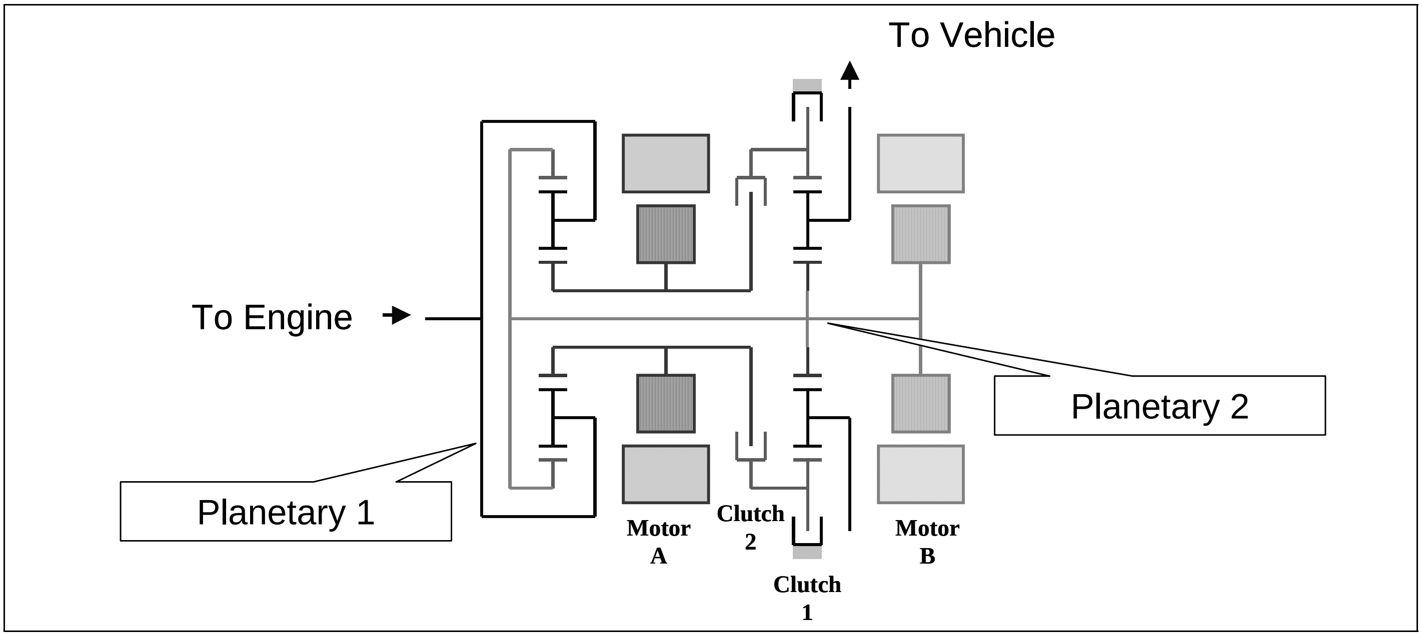

Figure 1 - Stick Diagram of gearing, clutches, and electric machines in DM-EVT

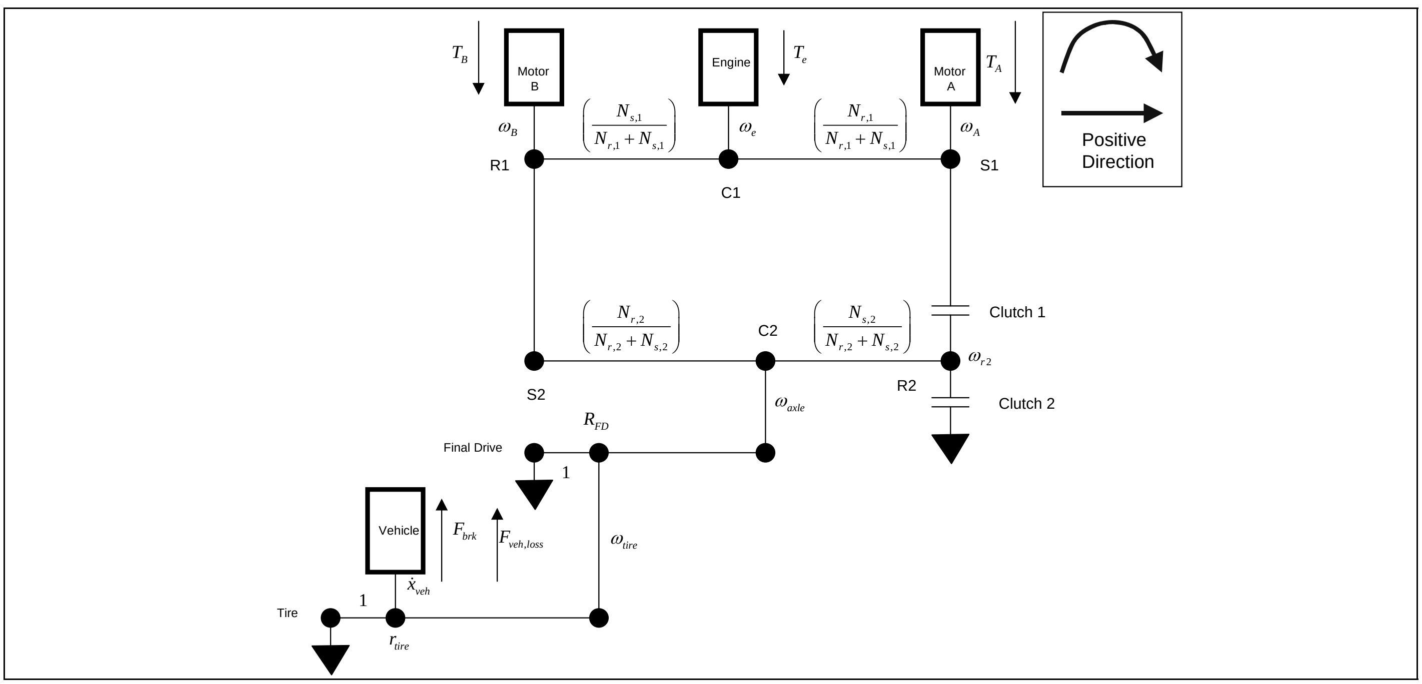

Figure 2 - Lever Diagram of Kinematics in the DM-EVT HEV Model

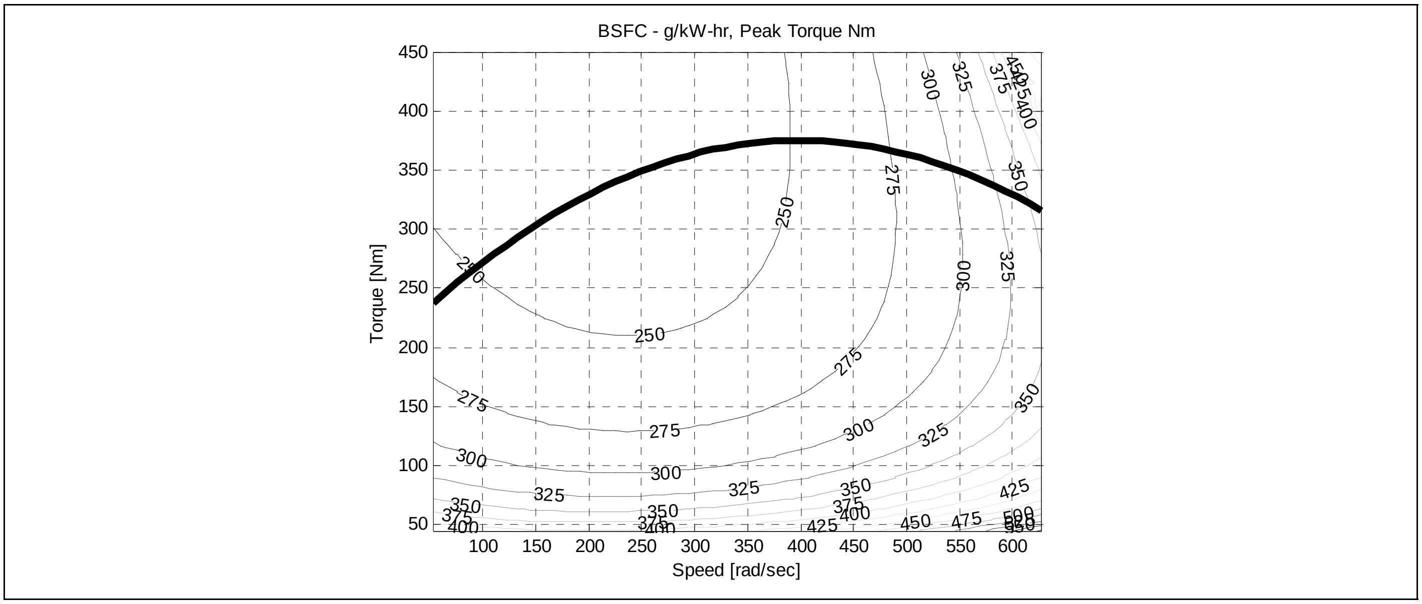

Figure 3 - Engine BSFC and Peak Torque Curves